Karhunen–Loève decomposition approach to analyzing complex network synchronization

2009 J. Phys. A: Math. Theor. 42 325101

(http://iopscience.iop.org/1751-8121/42/32/325101)

IOP PUBLISHING JOURNAL OF PHYSICS A: MATHEMATICAL AND THEORETICAL

J. Phys. A: Math. Theor. **42** (2009) 325101 (13pp) doi:10.1088/1751-8113/42/32/325101

Karhunen–Loève decomposition approach to analyzing complex network synchronization

Tao Jin[1], **Xiaoling Jin**[1], **Guanrong Chen**[2] **and Zhilong Huang**[1,3]

[1] Department of Mechanics, Zhejiang University, Hangzhou 310027, People's Republic of China
[2] Department of Electronic Engineering, City University of Hong Kong, People's Republic of China

E-mail: zlhuang@zju.edu.cn

Received 21 May 2009
Published 24 July 2009
Online at stacks.iop.org/JPhysA/42/325101

Abstract

In this paper, the approach of the Karhunen–Loève decomposition, known also as the proper orthogonal modes (POMs), is taken to analyze phase synchronization of various complex networks with different topologies, namely the classic Kuramoto model, coupled chaotic maps with Gaussian delays and a chain of diffusively coupled bistable oscillators. In the case of the Kuramoto model, the POMs reveal the tendency and the level of synchronization with the increase of the coupling strength for globally coupled networks and scale-free networks, while periodic POMs are found in nearest-neighbor coupled networks. Furthermore, for cluster networks on the Kuramoto model, the first leading POMs based on different time intervals reveal that different sub-groups of nodes synchronize gradually to different levels, eventually leading to the complete phase synchronization. In the case of coupled chaotic maps, some properties of phase synchronization change with the coupling strength value. In the case of the chain of diffusively coupled bistable oscillators, several main POMs not only determine the network phase synchronization but also provide good reconstruction of the network responses.

PACS numbers: 05.45.Xt, 05.45.Tp, 87.19.In

(Some figures in this article are in colour only in the electronic version)

1. Introduction

Synchronization is an interesting phenomenon, which plays a very important role in many fields such as physics, chemistry, biology, engineering, meteorology, economics and sociology [1–4]. On the other hand, complex networks have received a great deal of attention in the past

[3] Author to whom any correspondence should be addressed.

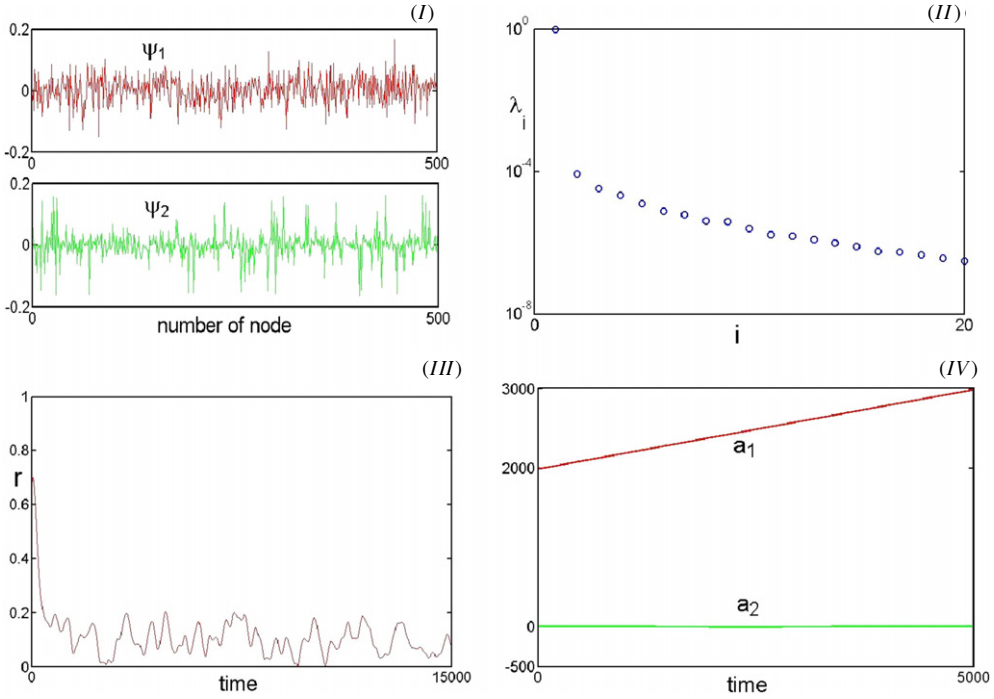

Figure 1. K–L decomposition for globally coupled networks with coupling strength $c = 1$. (*I*) The first and second POMs Ψ_i. (*II*) The largest 20 eigenvalues λ_i. (*III*) The amplitude or order parameter (7). (*IV*) The first and second coefficients $a_i(t_k)$.

decade. Synchronization of complex networks, consequently, was studied extensively in the past from different approaches [5–10]. The present paper takes a new approach based on the classic Karhunen–Loève (K–L) decomposition technique.

The K–L decomposition is a powerful tool for capturing the correlation between sequences of data sets, extracting pertinent information with only a small number of modes [11]. This technique can be used for order reduction by projecting higher dimensional data into a lower dimensional space, and can also be applied to feature extraction by revealing relevant but perhaps unexpected unknown structures hidden in the data. The key idea of this methodology is to reduce a large number of interdependent variables to a much smaller number of uncorrelated variables while retaining as much as possible the essential variation in the original variables [12]. The most striking property of the K–L decomposition is its optimality in the sense that it minimizes the average squared distance between the original signal and its reduced linear representation, which means that no other linear expansion may lead to a better representation of the underlying system with the same number of modes [13]. This method can be conveniently used to predict some basic and important properties of responses of higher dimensional linear as well as nonlinear systems. The mathematical formulation of the K–L decomposition was provided in, for example, [12], where it was also shown how to apply the technique to discrete systems. The eigenvalues (called proper orthogonal values), calculated from the autocorrelation matrix based on the data information from the underlying system, indicate the energy captured by their corresponding eigenvectors, called proper orthogonal modes (POMs), in which the few leading POMs are particularly important because they capture most of the energy. The leading POMs can

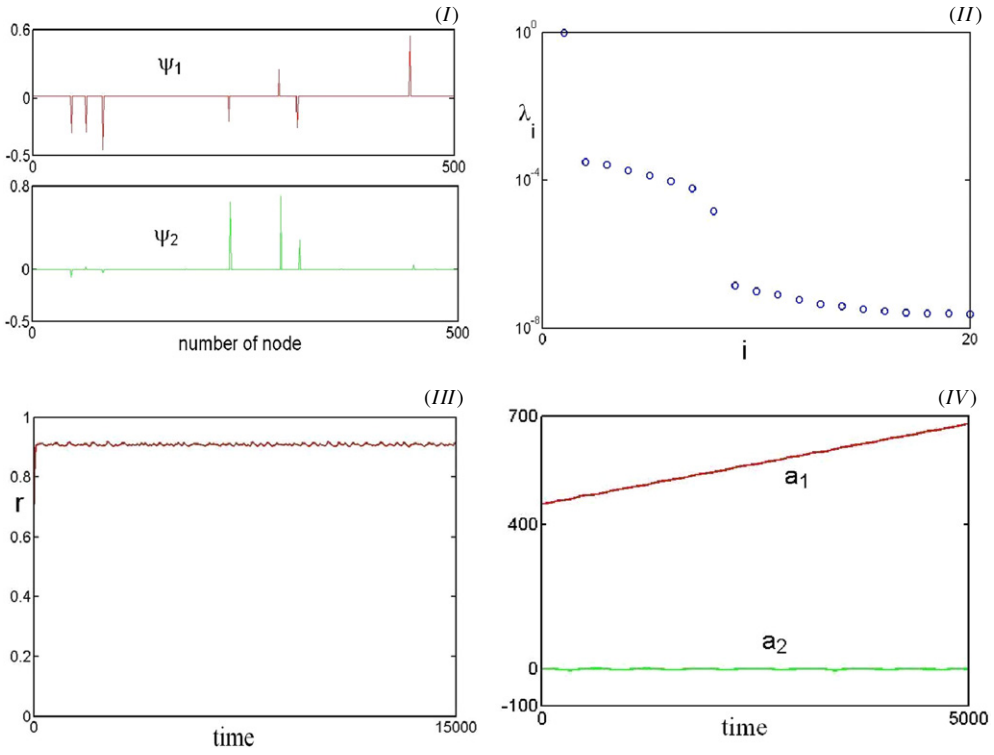

Figure 2. K–L decomposition for globally coupled networks with $c = 2.5$. All definitions are as in figure 1.

also reveal the relationship among all system variables (network nodes) and be used to reconstruct the approximate responses of the system. The K–L decomposition has been used in different fields for numerous applications, such as highly nonlinear conduction problems in structures made of periodic heterogeneous materials [11], model reduction of general nonlinear dynamical systems [14], dynamical behavioral analysis of coupled fiber laser oscillators with time delays [15] and continuous systems with infinite degrees of freedom that undergo vibroimpacts [16]. Moreover, the acceleration techniques for reduced-order models are based on the K–L decomposition [17], and some other applications [18–22].

2. The Karhunen–Loève decomposition approach

To introduce the procedure of the K–L decomposition, suppose that the dynamical response of a dynamical system is calculated numerically, with the response matrix given by

$$X = \begin{bmatrix} x_1(t_1) & \cdots & x_N(t_1) \\ \vdots & \ddots & \vdots \\ x_1(t_M) & \cdots & x_N(t_M) \end{bmatrix}, \tag{1}$$

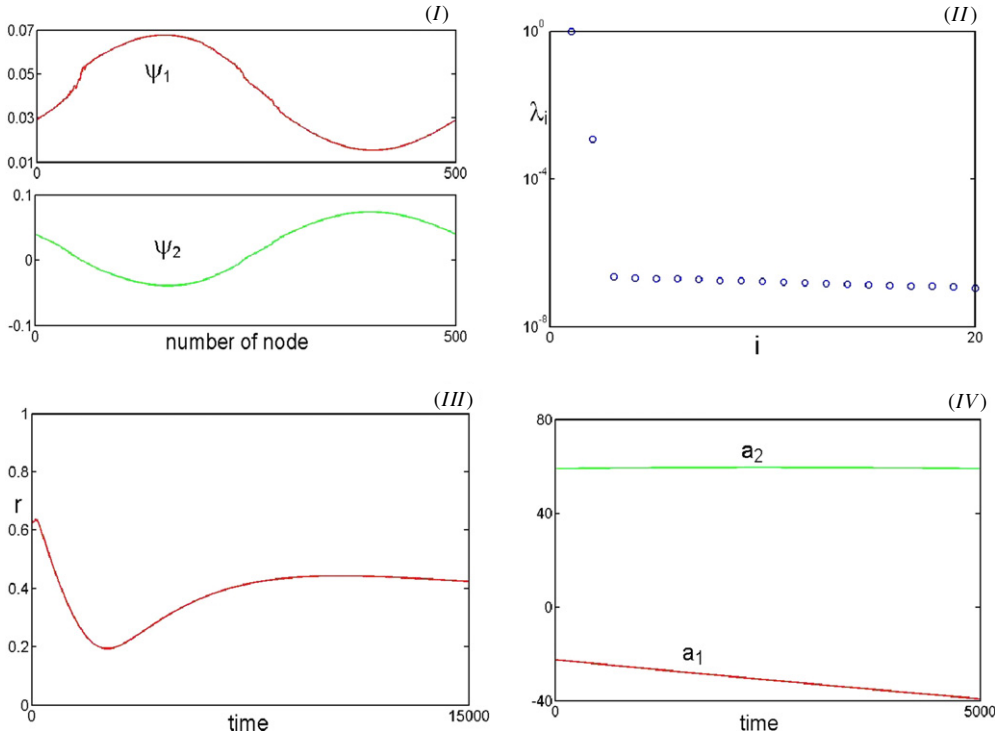

Figure 3. K–L decomposition for nearest-neighbor coupled networks with $c = 150$ and $k = 20$. All definitions are as in figure 1.

where N denotes the number of nodes in the system and M is the number of time steps of the evolution of the dynamical system. The associated matrix of mean values is

$$X_E = \frac{1}{M}\begin{bmatrix} \sum_{i=1}^{M} x_1(t_i) & \cdots & \sum_{i=1}^{M} x_N(t_i) \\ \vdots & \ddots & \vdots \\ \sum_{i=1}^{M} x_1(t_i) & \cdots & \sum_{i=1}^{M} x_N(t_i) \end{bmatrix}. \tag{2}$$

Moreover, the deviation matrix is defined by $X_d = X - X_E$, and the autocorrelation matrix is

$$R = \frac{1}{M} X_d^T X_d, \tag{3}$$

where R is symmetric and positive semi-definite. In addition, the associated eigenvectors or the K–L modes Ψ_i and eigenvalues λ_i of the system are obtained as

$$R\Psi = \Lambda\Psi \tag{4}$$

where $\Psi = [\Psi_1, \ldots, \Psi_N]$, $\Lambda = \mathrm{diag}(\lambda_1, \ldots, \lambda_N)$. Suppose also that the eigenvalues are arranged as $\lambda_1 \geqslant \lambda_2 \geqslant \cdots \geqslant \lambda_N$. The p-dominant eigenvalues satisfy $\left(\sum_{i=1}^{p} \lambda_i\right)/\left(\sum_{i=1}^{N} \lambda_i\right) \geqslant 0.999$, where this value of p is useful for estimating the dimensionality of the system in consideration. The p-dominant eigenvalues can also be used to reconstruct the approximate responses $\tilde{x}_j(t_k)$ of the system, which is written as an expansion in terms of eigenvectors $\Psi_i(j)$:

$$\tilde{x}_j(t_k) = \sum_{i=1}^{p} a_i(t_k)\Psi_i(j), \tag{5}$$

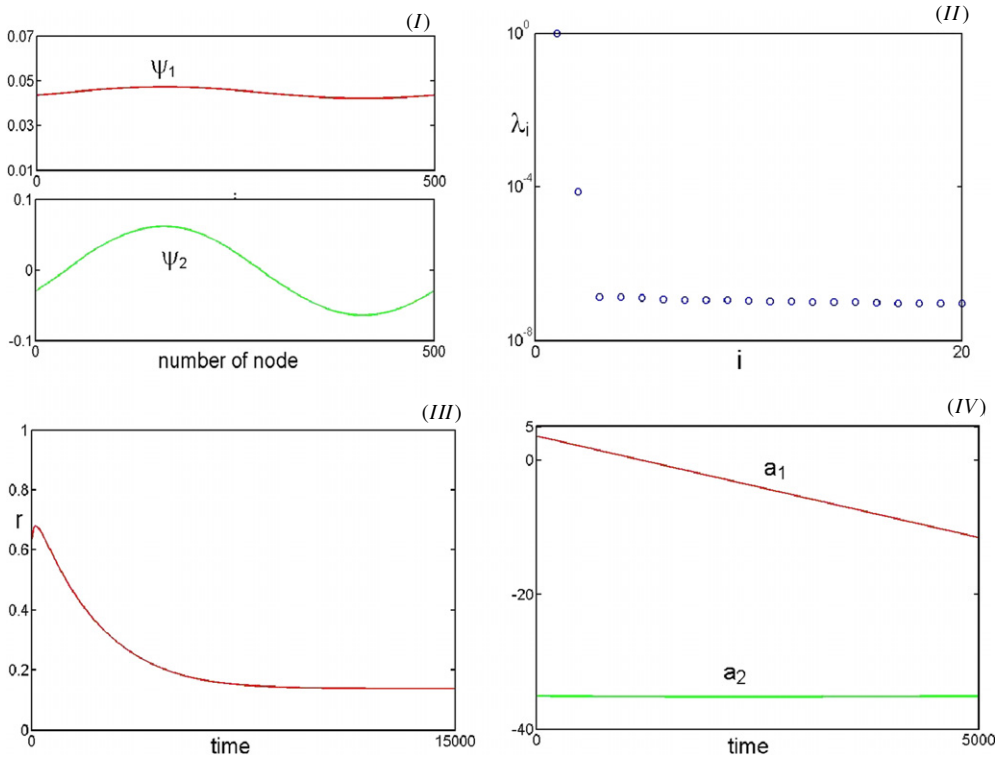

Figure 4. K–L decomposition for nearest-neighbor coupled networks with $c = 280$ and $k = 20$. All definitions are as in figure 1.

where j is the index number of a node and the coefficient $a_i(t_k)$ as a function of time is calculated by $a_i(t_k) = \sum_{j=1}^{N} x_j(t_k)\Psi_i(j)$, which weights the impact of the corresponding mode [17].

3. Analyzing complex network synchronization

The basic procedure of the K–L decomposition presented in section 2 will be adopted in the studies of network synchronization for three typical cases, as further discussed below, respectively.

3.1. Network I. The Kuramoto model

The Kuramoto model consists of N coupled phase oscillators, $\theta_i(t)$, $i = 1, 2, \ldots, N$, described by [23]:

$$\dot{\theta}_i = \omega_i + \sum_{j=1}^{N} \Gamma_{ij}(\theta_j - \theta_i), \qquad i = 1, \ldots, N, \tag{6}$$

where ω_i denotes the frequencies and Γ_{ij} represents the connectivity of the coupled system. Here, the natural frequencies ω_i satisfy a Gaussian distribution with zero mean and standard

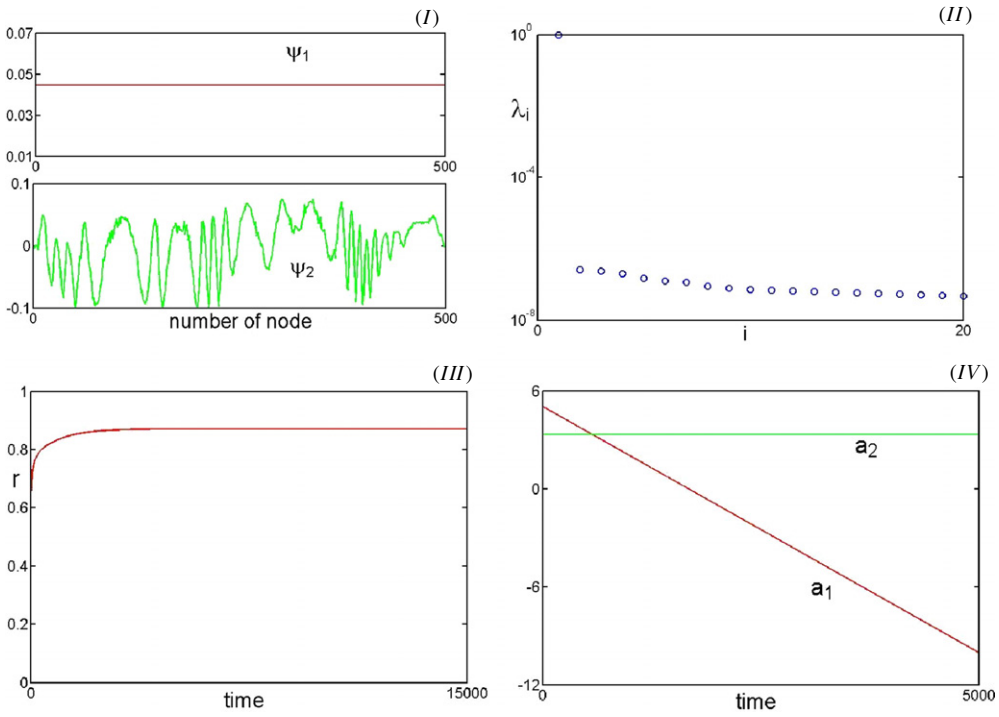

Figure 5. K–L decomposition for nearest-neighbor coupled networks with $c = 900$ and $k = 20$. All definitions are as in figure 1.

deviation 1. The phase synchronization is usually checked via the order parameter defined by [23]

$$r\,\mathrm{e}^{\mathrm{i}\varphi} = \frac{1}{N}\sum_{j=1}^{N}\mathrm{e}^{\mathrm{i}\theta_j}, \tag{7}$$

where r and φ are the amplitude and phase of the order parameter, respectively, and the level of synchronization is measured by the amplitude r, in the sense that $r = 1$ means complete synchronization in phase and $r = 0$ means completely unsynchronized.

Four kinds of network topologies are simulated based on the Kuramoto model.

(i) The first one is a globally coupled network with the same coupling strength c, i.e.

$$\Gamma_{ij}(\theta_j - \theta_i) = \frac{c}{N}\sin(\theta_j - \theta_i). \tag{8}$$

(ii) The second one is a nearest-neighbor coupled network, i.e. all the nodes are arranged as in circle and every node is connected to $k/2$ (k is an even integer) nearest nodes at both sides of it, as follows:

$$\Gamma_{ij}(\theta_j - \theta_i) = \frac{c}{N}e(i,j)\sin(\theta_j - \theta_i), \tag{9}$$

where $e(i, j) = e(j, i) = 1$ if there is a connection between node i and node j, but it is zero otherwise.

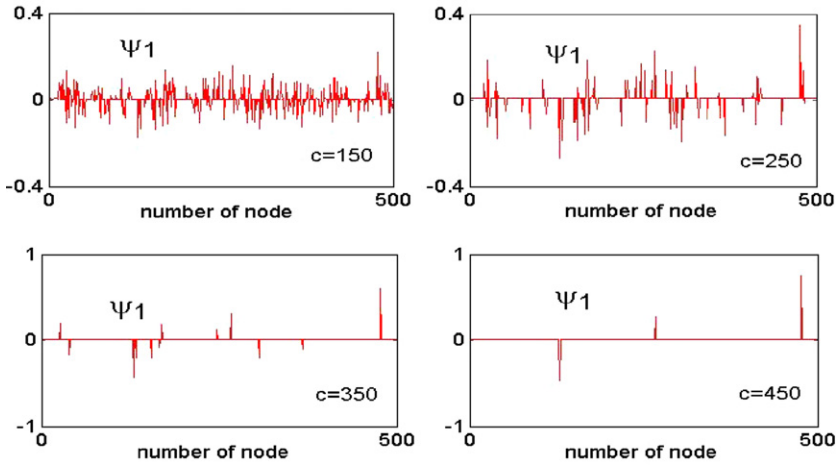

Figure 6. The leading POMs for scale-free networks with different coupling strengths.

(iii) The third one is a scale-free network in the same form as (9). Initially, ten nodes are randomly coupled; then, at each time step, a node is being added into the network and it brings in three new links to preferentially connect to three randomly selected existing nodes until the total number of nodes is 500; then the process is stopped. Here, the preferential probability that the new node is connected to the existing node j in the network is $k_j / \sum_l k_l$, where k_j denotes the degree of node j [24].

(iv) The fourth one is a cluster network in the same form as (9). In this network, a total of 400 nodes are equally divided into four sub-groups. Each sub-group of 100 nodes is a small globally coupled sub-network. Then, eight nodes from sub-group 1 are randomly selected and completely coupled to randomly selected eight nodes in sub-group 2; meanwhile, eight nodes from sub-group 3 are randomly selected and completely coupled to randomly selected eight nodes in sub-group 4. Finally, two nodes in each sub-group are randomly selected and then coupled completely. A relation between the spectral information of the Laplacian matrix and the hierarchical process of the emergence of communities at different time scales was reported in [25]. In this paper, this problem is further studied, with a more detailed analysis and discussions, by using the proposed procedures of the K–L decomposition.

The POMs Ψ_i, eigenvalues λ_i and coefficients a_i for different networks are calculated, as shown in figures 1–7, where $N = 500$ was used for globally coupled, nearest-neighbor coupled and scale-free networks, while $N = 400$ was used for cluster networks.

It can be seen from figure 1 that, with a small coupling strength for the globally coupled network, the first and second POMs are irregular and the order parameter r is very close to zero, which both demonstrate that the oscillators cannot synchronize with each other in phase. As the coupling strength increases, more and more oscillators get into the phase of synchronization.

It can be observed from figure 2 that the first leading POM and the values of the order parameter r both indicate that most nodes become synchronized. Furthermore, the first leading POM clearly shows that the nodes are not synchronizing, but this phenomenon is not reflected by the value of the order parameter r.

It can be seen from figure 3 that with a small coupling strength for the nearest-neighbor coupled network, the first and second POMs are periodic and the order parameter r is far from 1,

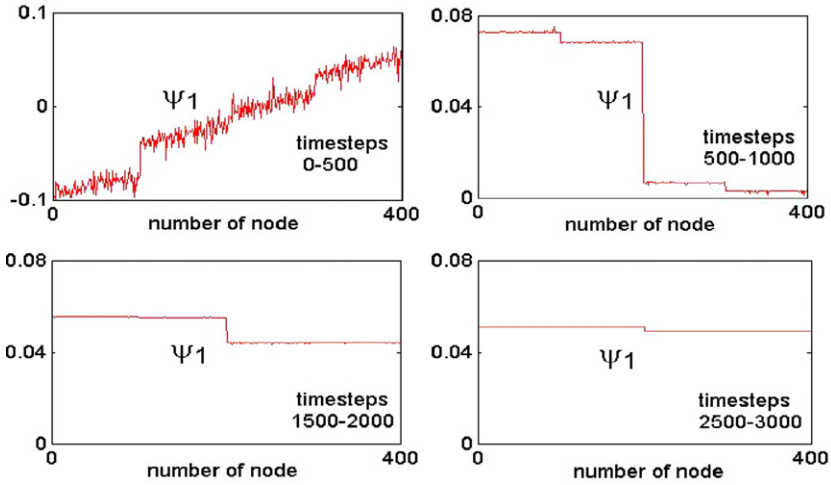

Figure 7. The leading POMs for cluster networks on different time intervals. The coupling strength $c = 12$.

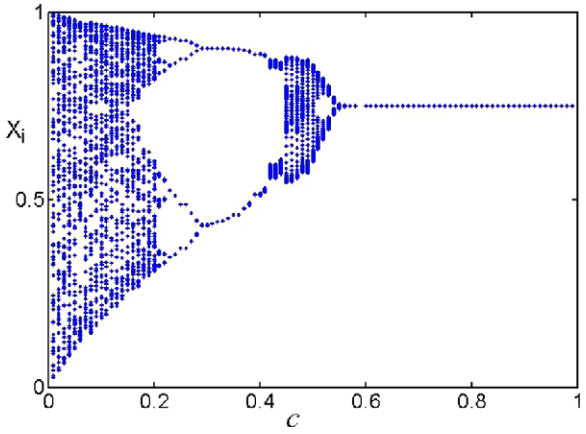

Figure 8. Bifurcation diagram of the network response versus the coupling strength c: $N = 500$, $\tau_0 = 3$, $d = 2$.

which means that the system is not synchronized. It can also be seen from figure 4 that the order parameter r decreases as the coupling strength increases. This is because the second coefficient $a_2(t_k)$ in figure 4(*IV*) and the associated periodic second mode in figure 4(*I*) are dominant and the periodic oscillations of all nodes significantly reduce the order parameter and the synchronizability of the system. With a further increase in the coupling strength, the order parameter r becomes gradually closer to 1 and the periodic POMs disappear eventually, as shown in figure 5. To the best of the authors' knowledge, the phenomenon of periodic oscillations among all nodes in a nearest-neighbor coupled network is observed and reported for the first time here by using the K–L decomposition method, and this phenomenon cannot be explained by using the order parameter r alone.

It can also be seen from figures 1–5 that the leading (normalized) eigenvalues and the corresponding coefficients are all much larger than the others in most cases, which verifies once again that the leading K–L modes are indeed the dominant modes.

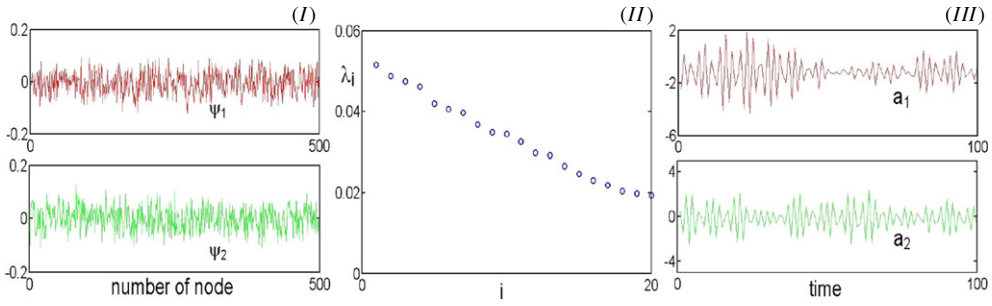

Figure 9. The K–L decomposition of the network with coupling strength $c = 0.1$. (*I*) The first and second POM; (*II*) The largest 20 eigenvalues; (*III*) The first and second coefficients $a_i(t_k)$ of the POMs.

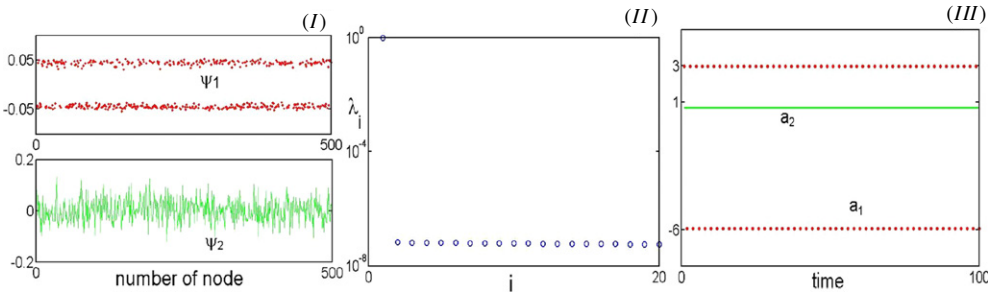

Figure 10. The K–L decomposition of the network with coupling strength $c = 0.35$. All definitions are as in figure 9.

The POMs with different coupling strengths in scale-free networks are presented in figure 6. It can be observed that the first-mode curve becomes flat as the coupling strength becomes larger, demonstrating that the system gets into the phase of synchronization. The percentages of the corresponding eigenvalues λ_1 of these first POMs are all larger than 99.9%, i.e. $\lambda_1 / \left(\sum_{i=1}^{500} \lambda_i\right) > 0.999$.

The first POMs obtained based on the data over different time intervals of the cluster networks are plotted in figure 7. The percentages of the corresponding eigenvalues λ_1 of these first POMs, over five time intervals, are 95.02%, 99.51%, 99.87%, 99.981% and 99.9996%, respectively. It can be seen from figure 7 that the four sub-groups get into the phase of synchronization individually on the time interval [500, 1000]; then, the combined first and second sub-groups and the combined third and fourth sub-groups both get into the phase of synchronization individually on the time interval [1000, 1500]; finally, the whole system achieves synchronization on the time interval [2000, 2500]. These demonstrate that the leading POMs on different time intervals can indeed reveal the detailed processes of synchronization of the networks. It should be pointed out that even though a similar phenomenon has been reported in [25] in a different model, the detailed process evolving to synchronization of the system can be observed more directly and more clearly by using the K–L decomposition method.

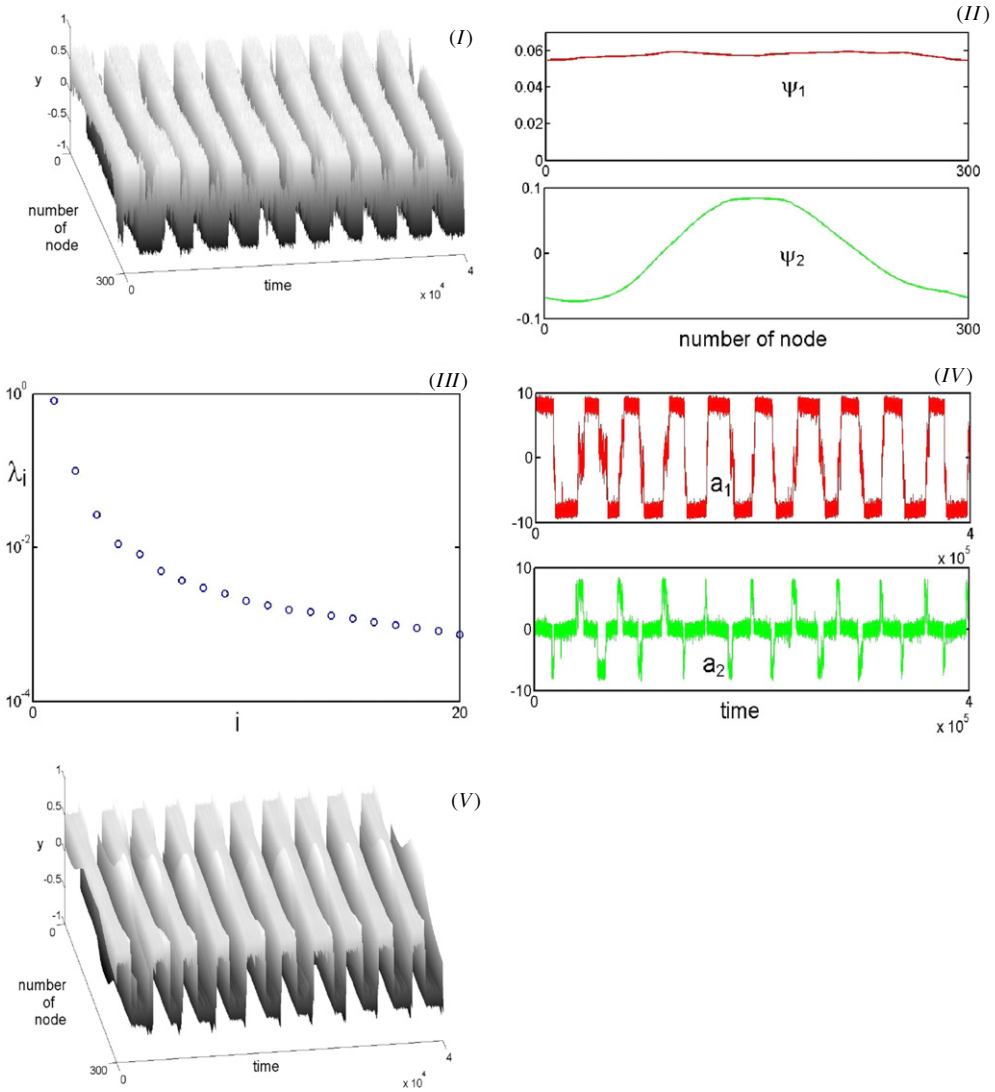

Figure 11. K–L decomposition of the network with periodic boundary condition: $N = 300$, $M = 50, k = 125, K = 15, D = 0.1, m = 0.25$. (*I*) Original responses of the system (11). (*II*) The first and second POMs. (*III*) The largest 20 eigenvalues. (*IV*) The first and second coefficients $a_i(t_k)$ of POMs. (*V*) Reconstructed responses using the first and second POMs.

3.2. Network II. Coupled chaotic maps with Gaussian delays

Consider N coupled chaotic maps with time delays, described by [26]

$$x_i(t+1) = (1-c)f[x_i(t)] + \left\{ c \sum_{j=1}^{N} e(i,j) f[x_j(t-\tau_{ij})] \right\} \Big/ b_i, \tag{10}$$

where t and i are discrete indices of time and space, respectively, $f(x) = mx(1-x)$ is the chaotic logistic map, $e(i, j)$ is the connectivity matrix of the network as defined in network I above, c is the coupling strength, τ_{ij} is the time delay in the interaction between node i and

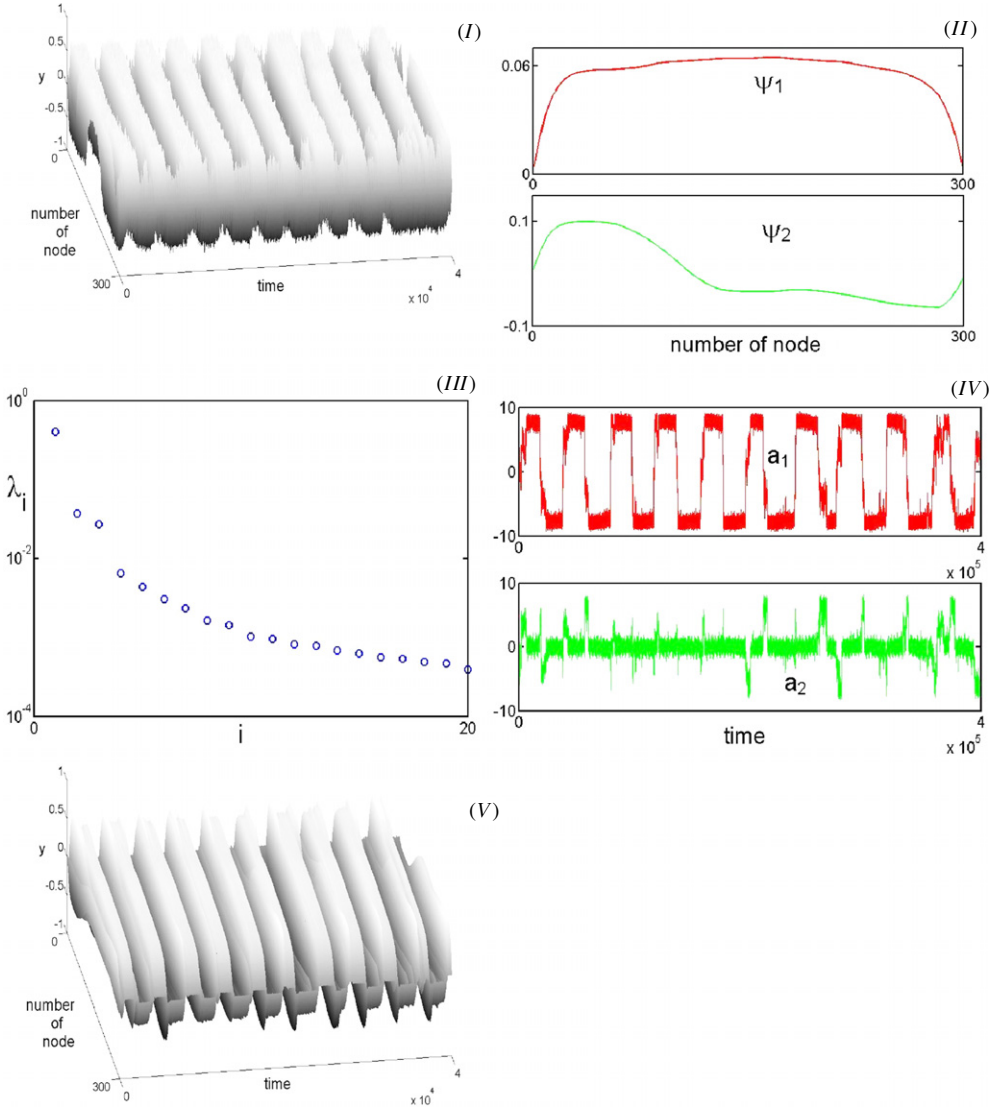

Figure 12. K–L decomposition of the network with fixed boundary condition. All definitions are as in figure 11.

node j satisfying $\tau_{ij} = \tau_0 + \mathrm{Near}(\mathrm{d}\xi)$ [26], where d is a real constant, ξ is a Gaussian random variable with zero mean and standard deviation 1, and Near(dξ) means the integer nearest to the value of dξ (the distribution of delays has to be truncated to avoid becoming negative), and $b_i = \sum_j e(i, j)$ is the degree of the node i, $i, j = 1, 2, \ldots, N$. The network has a small-word topology, generated from the nearest-neighbor network with $k = 6$ and $p = 0.3$ [24].

It can be seen from figure 9 that the first and second POMs are irregular and the largest 20 eigenvalues have the same order in magnitude when the coupling strength is small. It implies that the first POM is not the dominant mode in the present case and the responses of the system are random.

It can be seen from figure 10 that the first POM has two possible responses from the network and the largest eigenvalue is the dominant one. Clearly, the behavior of the K–L decomposition agrees well with the network bifurcation behavior shown in figure 8.

3.3. Network III. A chain of oscillators

A chain of overdamped oscillators with diffusive coupling (constant strength $K > 0$) and a bistable potential $V(y) = -my^2/2 + y^4/4$, as studied in [27], is described by

$$\dot{y}_n = K\Delta y_n - V'(y_n) + \sqrt{2D}\xi_n(t) + S_n^{(M_k)}(t), \qquad n = 1, \ldots, N, \tag{11}$$

where $\Delta y_i = y_{i+1} - 2y_i + y_{i-1}$, $V'(y)$ denotes the derivation of y, $\xi_n(t)$ is a sequence of independent Gaussian white noise with zero mean and intensity D, $S_n^{(M_k)}(t) = \{s(t)$ if $n \in M$, or 0 otherwise$\}$, $s(t) = A\cos(\omega t)$ with $A = 0.025$ and $\omega = 5\pi \cdot 10^5$, and $M_k = \{k+1, k+2, \ldots, k+M\}, 0 \leqslant M \leqslant N$. Two different boundary conditions are considered:

(1) periodic boundary condition: $\Delta y_1 = y_2 - 2y_1 + y_N$, $\Delta y_N = y_1 - 2y_N + y_{N-1}$;
(2) fixed boundary condition: $\Delta y_1 = y_2 - 2y_1$, $\Delta y_N = y_{N-1} - 2y_N$.

In numerical simulations, the time step is 0.01 and the data of 40 million stationary time series are used for computing the K–L decomposition. The responses of the network and the results of the K–L decomposition for the two boundary conditions are shown in figures 11 and 12, respectively.

It can be seen from figures 11 and 12 that the phenomenon of spatiotemporal stochastic resonance is observed for the network with both boundary conditions. The first POM of the network is the dominant mode and the largest eigenvalue is the key eigenvalue in using the K–L decomposition for this investigation. It can also be seen from figures 11(V) and 12(V) that the reconstruction by using the first and second POMs as shown in (5) represents the basic behavior of the responses of the network, for both the two cases with different boundary conditions.

4. Conclusions

In this paper, the K–L decomposition has been applied to study the synchronization of dynamical responses of various complex networks. The methodology has been used to predict the behavior of the Kuramoto model, coupled chaotic maps and a chain of oscillators with bistable potential, in different structural topologies. It is found from this study that the first leading POM not only is the key mode of the responses of the network in most cases, but also reveals the detailed processes of synchronization of the network over different time intervals. The phenomenon of periodic oscillations among all nodes in the nearest-neighbor coupled network is observed and reported for the first time in this paper. The first and second POMs are dominant in many cases, which were used to reconstruct a good approximate response of the chain of oscillators with a bistable potential. All the results have demonstrated that the K–L decomposition is indeed a powerful tool for investigating the dynamical behavior of various complex networks and systems.

Acknowledgments

The work reported in this paper was supported by the National Natural Science Foundation of China under grant nos 10672142 and 50890174, a special research fund for the Doctoral

Program of High Education of China under grant no 20070335053 and the City University of Hong Kong under the SRG grant 7002274.

References

[1] Rosa E, Ott E and Hess M H 1998 *Phys. Rev. Lett.* **80** 1642
[2] Stark J and Hardy K 2003 *Science* **29** 1192
[3] Pikovsky A, Rosenblum M and Kurths J 2001 *Synchronization* (Cambridge: Cambridge University Press)
[4] Osipov G V, Kurths J and Zhou C 2007 *Synchronization in Oscillatory Networks* (Berlin: Springer)
[5] Wang X F 2002 *Int. J. Bifurcation Chaos* **12** 885
[6] Barahona M and Pecora L M 2002 *Phys. Rev. Lett.* **89** 054101
[7] Earl M G and Strogatz S H 2003 *Phys. Rev.* E **67** 03624
[8] Li X, Jin Y Y and Chen G R 2003 *Physica* A **328** 287
[9] Sorrentino F and Ott E 2008 *Phys. Rev. Lett.* **100** 114101
[10] Hwang D U, Chavez M, Amann A and Boccaletti S 2005 *Phys. Rev. Lett.* **94** 138701
[11] Monteiro E, Yvonnet J and He Q C 2008 *Comput. Mater. Sci.* **42** 704
[12] Kerschen G, Golinval J, Vakakis A F and Bergman L A 2005 *Nonlinear Dyn.* **41** 147
[13] Trindade M A, Wolter C and Sampaio R 2005 *J. Sound Vib.* **279** 1015
[14] Bogner T 2007 *Phys. Rev.* E **76** 056707
[15] Franz A L, Roy R, Shaw L B and Schwartz I B 2007 *Phys. Rev. Lett.* **99** 053905
[16] Azeez M F A and Vakakis A F 2001 *J. Sound Vib.* **240** 859
[17] Cizmas P G A, Richardon B R, Brenner T A, O'brien T J and Breault R W 2008 *J. Comput. Phys.* **227** 7791
[18] Holmes P, Lumley J L and Berkooz G 1996 *Turbulence, Coherent Structures, Dynamical Systems and Symmetry* (New York: Cambridge University Press)
[19] Han S and Feeny B F 2003 *Mech. Syst. Signal Process.* **17** 989
[20] Graham M D and Kevrekedis I G 1996 *Comput. Chem. Eng.* **20** 495
[21] Feeny B F 2002 *J. Vib. Acoust.* **124** 157
[22] Ma X and Vakakis A F 1999 *AIAA J.* **37** 939
[23] Acebrón J A, Bonilla L L, Pèrez C J, Ritort F and Spigler E 2005 *Rev. Mod. Phys.* **77** 137
[24] Boccaletti S *et al* 2006 *Phys. Rep.* **424** 175
[25] Arenas A *et al* 2006 *Phys. Rev. Lett.* **96** 114102
[26] Masoller C and Martí A C 2005 *Phys. Rev. Lett.* **94** 134102
[27] Samoletov A, Chaplain M and Levi V 2004 *Phys. Rev.* E **69** 045102